

Accelerator physics model of expected beam loss along the SNS accelerator facility during normal operation

**N. Catalan-Lasheras (Ed.), J. Galambos, N. Holtkamp
D. Raparia, R. Shafer, J. Staples, J. Stovall,
E. Tanke, T. Wangler, J. Wei**

March 29, 2001

1 Introduction

The most demanding requirement in the design of the SNS accelerator chain is to keep the accelerator complex under hands-on maintenance. This requirement implies a hard limit for residual radiation below 100 mrem/hr at one feet from the vacuum pipe and four hours after shutdown for hundred days of normal operation. The final level of radiation at the time at places of access will determine the time limitation for repairs and service.

It has been shown by measurements as well as simulation [1] that the limit on the beam loss imposed by hands-on maintenance corresponds to 1-2 Watts/meter average beam losses. This loss level is achievable all around the machine except in specific areas where remote handling will be necessary. These areas have been identified and correspond to collimation sections and dumps where a larger amount of controlled beam loss is foreseen.

Even if the average level of loss is kept under 1 W/m, there are circumstances under which transient losses occur in the machine. During commissioning, tune-up or element failure, losses above the average may take place. The prompt radiation or potential damage in the accelerator components can not be deduced from an average beam loss of 1 W/m.

At the same time, controlled loss areas require a dedicated study to clarify the magnitude and distribution of the beam loss. This information is essential for designing harder components, the shielding around them, their removal procedures or the access locations to give some examples.

From the front end to the target, we estimated the most probable locations for transient losses and give an estimate of their magnitude and frequency. This information is useful to calculate the necessary shielding or determine the safety procedures during machine operation.

In this report we only evaluate expected beam loss under normal operation. Loss incurred due to system failure will be documented in a separate report.

2 Controlled losses

Controlled losses occur at the choppers, in the LEBT and MEBT lines, at the collimators in the HEBT, Ring and RTBT and in the three dumps along the accelerator. In most of these sections remote handling is necessary and specific shielding and other protection measures should be implemented according to the final radiation levels.

2.1 Front end

The 1 msec beam pulse from the ion source is chopped in the LEBT at 65 keV. Assuming the LEBT chopper rise time is infinitely fast, $(100-68)=32\%$ would be lost on the LEBT chopper target or in the RFQ. However, due to the $t \leq 50$ nsec rise/fall of the LEBT chopper, only 27.7% of the beam is lost at the end of the LEBT at 65 keV.

After acceleration and bunching in the RFQ, a second chopper is located in the MEBT to clean the unbunched beam. Had the MEBT copper rise time be infinitely fast, $(32-27.7)=4.3\%$ would be lost on the MEBT chopper target at 2.5 MeV. The actual rise/fall time is about 10 ns and an antichopper is used to compensate partially kicker beam. The beam extinction is better than 10^{-4} .

2.2 HEBT transverse collimators

To collimate the linac beam we use charge exchange movable carbon foils which strip the H^- to H^+ . The H^+ beam is separated from the H^- beam by the magnets and hits the front face of the absorbers

downstream [2]. The stripper foils are located at 13σ becoming the main aperture restriction in the line. Assuming a Gaussian beam profile coming from the Linac, the tails intercepted by the cleaning system will account for a fraction of 10^{-5} of the total beam. These losses will be distributed evenly between two absorbers.

The position and aperture of the foil and absorbers have been optimized to provide large impact parameters at the absorber.

Under nominal conditions the protons hit the absorber at a minimum distance of ≈ 4 mm from the vacuum pipe inner radius. The trace of the beam on the front of the absorber defined by the foil edge is shown in figure 1.

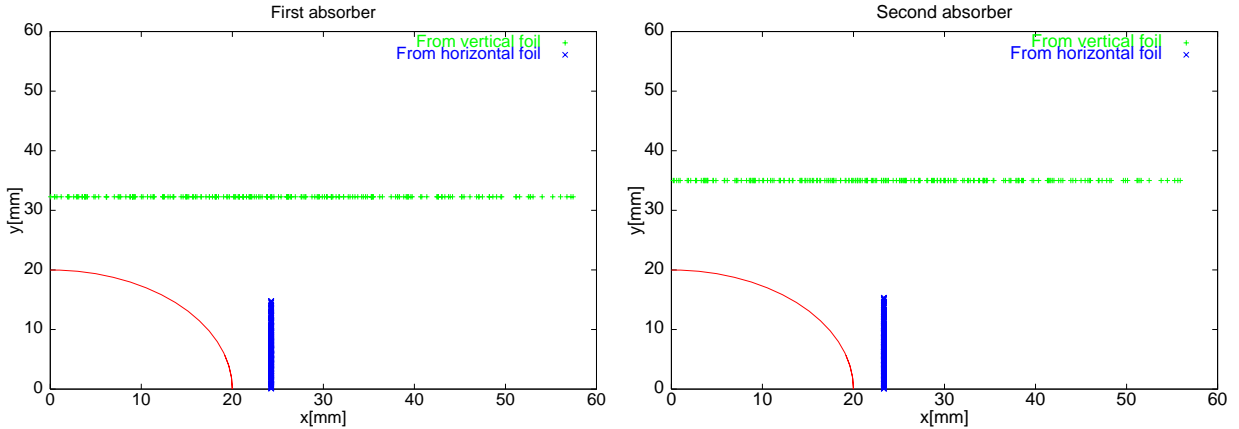


Figure 1: Transverse projection of the H^+ beam at the entrance of the collimator (red line). The horizontal line has been generated at the first vertical foil while the vertical line is generated at the horizontal foil.

Name	Aperture 13π [mm]	Impact Parameter	
		[mm]	[mrad]
Scraper 1 Up/Down	13	12.3	-5.9
Scraper 1 Left/Right	17	4.3	6.7
Scraper 2 Up/Down	13	15.0	-4.1
Scraper 2 Left/Right	17	3.3	6.1

Table 1: Nominal impact parameter and angle of the H^+ beam at absorbers 1 and 2 in the HEBT line

2.3 HEBT Longitudinal collimator

In a similar arrangement to the transverse collimation, a mobile stripping foil located in the achromat where dispersion is high, will dump the longitudinal halo onto an absorber located downstream. In this case, the collimator is external to the beam line and there is no protons lost along the line. This system will collimate off momentum particles in the linac beam including large energy spread and energy jitter. The maximum fraction of the beam in the tails has been estimated to be 10^{-3} of the total beam [3].

2.4 Ring collimation section

Losses in the ring are mainly produced by gradual emittance growth produced by space charge and magnet errors. With the introduction of a primary collimator, the incident angle is increased but not enough to reach the front face of the secondary collimators. The losses are produced along the inner surface of the vacuum pipe. The impact angle takes typical values between 0 and 10 mrad.

A preliminary distribution of the losses along the collimation section (superperiod B) has been made with the program K2. Figure 2 shows the fraction of beam absorbed in every collimator as well as quadrupoles and free drifts [4].

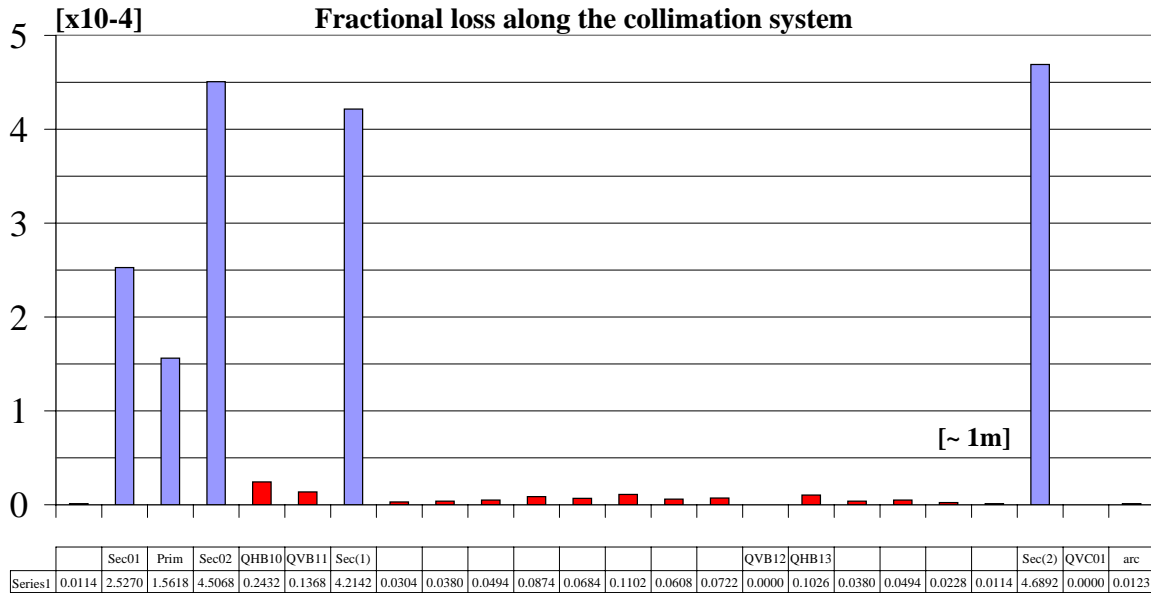


Figure 2: Loss distribution along the collimation straight section. The data are fractional loss assuming a total loss of $1.9 \cdot 10^{-3}$.

2.5 RTBT collimators

The RTBT collimators are provided to protect the target and RTBT line against extraction kicker malfunction [5].

After collimation of the beam inside the ring, the extension of the beam is well defined at the RTBT line. Under nominal conditions, the beam passes through the line without touching the vacuum pipe. A failure of one of the fourteen extraction kickers will produce an orbit deviation along the RTBT line. However, no beam hits the vacuum pipe and the beam impacts the target at the nominal location. In the event of a failure of two kickers, approximately 10% of the beam hits the collimator with no further losses downstream. The losses are equally distributed between the two absorbers. In the rare case of more than two kicker failures, the whole pulse is dumped onto the two collimators. We estimate the average beam losses in the RTBT collimator by the probability of kicker failure and the fraction of beam collected at each scenario.

Nevertheless, we have to draw attention to the fact that prompt losses are high and very localized. The design of the collimators has been done to resist two whole consecutive pulses after which the machine should be stopped and the kickers fixed.

3 Uncontrolled losses

In this section, we review the areas with higher risk of uncontrolled losses. Under normal operation we do not expect losses above the design requirement of 1-2W/m.

To help identify hot spots in the machine, we have reviewed the main loss mechanisms for every accelerator section. The final value of loss and the location of losses comes from simulations, calculations and scaling from measurement data in other machines.

3.1 RFQ

The transmission in the RFQ structure is expected to be of the order of 80%. The other 20% of the beam will be lost along the cavity. We consider these losses uncontrolled because no special protection or shielding is provided. However, we do not expect any activation at this low energy ($E \leq 2.5$ MeV) and the area is assumed to fulfill the requirements for hands-on maintenance. In addition, this is an area with controlled access during operation.

For simulation purposes, we consider the loss homogeneously distributed along the RFQ inner surface (≈ 4 m).

3.2 LINAC

The main sources of loss in the linac are ionization and magnetic stripping as well as halo growth due to mismatch and space charge. Due to the level of loss we are interested in, and the large number of free input parameters in the beam dynamics simulation, the net amount of losses and their location is difficult to predict by simulation. We extrapolate our experience from other Linacs as LANSCE to predict the most probable loss locations and to confirm the required beam loss limit of 1W/m.

The comparison between the beam envelope and the vacuum pipe along the SNS linac is shown in Fig. 3 [7]. From this plot we can imply that localized losses may occur at the beginning of the DTL, at the end of the CCL and at the transition of between CCL and SCL. From experience in LANSCE and LEDA [8, 10], we know that losses typically occur at locations where a change in transverse focusing or RF frequency introduce a mismatch. In the SNS linac there is a frequency transition between the DTL and CCL where we expect losses above the average.

As for the superconducting linac the bore radius aperture is much larger than the nominal beam. In addition, the vacuum pressure is one order of magnitude lower than in the warm linac ($=10^{-9}$ compared to $5 \cdot 10^{-8}$). Simulations and stripping calculations give a negligible amount of losses. On the other hand, one should be very cautious with our expectations as there is no experience with superconducting proton linacs up to now. Measurements in the high energy end of the LANSCE linac, indicated unexplained losses up to 0.6W/m that have not been predicted by simulation [8].

It is foreseen to continue operating with a missing klystron in the superconducting linac. This operating mode creates a mismatch and populates the transverse tails of the beam [9] leading to

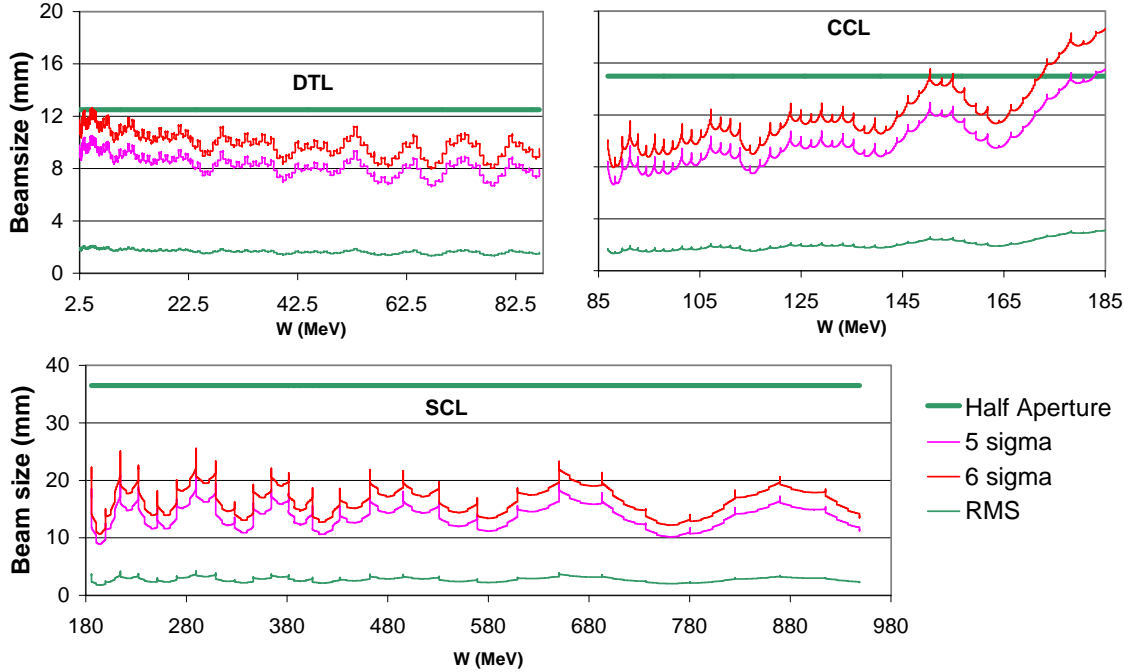


Figure 3: Envelope of the beam along the DTL, CCL and SCL. The minimum aperture of the vacuum pipe in every structure is indicated for comparison.

exceptional losses downstream from the missing cavity. Studies are in progress to establish the importance of these losses in the SNS cold linac.

The location of losses is easier to predict. In case of mismatch or abnormal emittance growth beam loss will be concentrated in the warm quadrupole sections where the aperture is smaller and the beam reaches its maximum extent. This assumption is supported by measurements made at LANSCE CCL where residual radiation at quadrupoles was found to be up to a factor 100 larger than the average.

We have estimates of the stripping losses which will account for a significant fraction of the average 1W/m along the linac especially in the low energy range where the stripping cross sections are larger. These calculations agree with measured data [6]. The vacuum stripping losses for the H^- beam depending on the energy are shown in figure 4. The losses, expressed in watt per meter assume a generic vacuum composition for warm sections and mainly hydrogen for the cold sections.

3.3 HEBT

Along the HEBT, the sources of uncontrolled loss are residual gas and magnetic stripping. As in the case of the Linac, these losses are homogeneously distributed along the line and inside the magnetic fields. At 1 GeV the cross section of H^- stripping is $9.14 \cdot 10^{-19} \text{ cm}^2$ and $1.30 \cdot 10^{-19} \text{ cm}^2$ for Nitrogen and Hydrogen respectively. With a vacuum of $5 \cdot 10^{-8}$, the fractional stripping losses account for $\approx 2.8 \cdot 10^{-5}$ along 170 meters or $1.6 \cdot 10^{-7}$ per meter. Magnet strength is chosen so that the magnetic stripping is at the 10^{-8} per meter level much lower than the vacuum stripping loss.

The efficiency of the transverse collimations has been estimated to an average of 92.5%. The

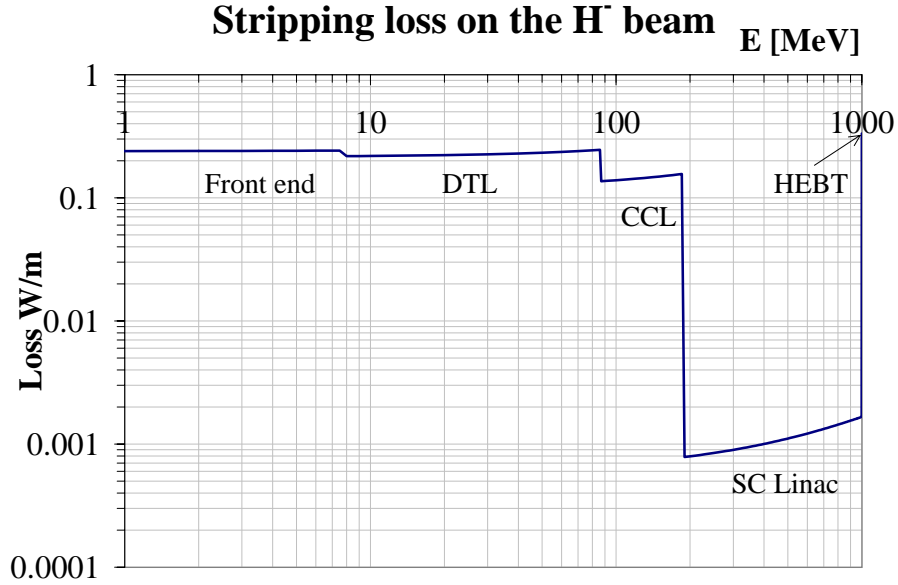


Figure 4: Residual gas stripping loss for H^- beam from the front end to the HEBT transfer line.

remaining protons will be spread along the downstream cells and the beginning of the achromat.

3.4 Injection Section

The main source of loss in the injection section is the nuclear scattering of the beam in the Carbon foil. Besides, we need to consider the magnetic stripping of the H^- beam in the second dipole of the injection chicane INJB2 where the H^- beam traverses an area close to the magnet coil.

The losses produced at the injection foil are dominated by nuclear scattering. Once the energy and foil thickness have been defined, the loss is determined by the size of the incoming beam and the painting scheme.

The maximum number of foil crossing has been estimated by simulation [4]. The average number of foil crossings per proton is ≈ 7 in nominal conditions. Yet, if the beam emittance increases or deviates from a Gaussian distribution, this number increases up to 12 crossings per proton. For a carbon foil of $300 \mu\text{g}/\text{cm}^2$, the fractional loss at the foil due to nuclear scattering will be $\approx 3.7 \cdot 10^{-5}$ under nominal conditions and up to $\approx 6.3 \cdot 10^{-5}$ for an exceptional large beam.

For the magnetic stripping we assume a magnetic field of 0.25-0.3 Tesla. For this magnetic field, $1.3 \cdot 10^{-7}$ of the beam will be lost along the effective magnetic length of the dipole (≈ 1 meter) [11].

3.5 Ring

Along the arcs and in the injection, extraction and RF straight sections we expect spurious losses arising from the inefficiency of the collimation system. A fraction of $2.0 \cdot 10^{-3}$ of the beam is in the tails and is intercepted by a collimation system with a minimum efficiency of 95%. The remaining $1.0 \cdot 10^{-4}$ of the beam form residual halo homogeneously distributed in phase-space. We assume

that this halo is spread according to the dispersion, phase advance and aperture along the 218 meters of the ring outside the collimation system.

3.6 RTBT

The losses along the RTBT line expected during normal operation are negligible. The only potential source of loss is the residual beam coming from the RTBT collimators expected to be $\leq 10\%$ of the incident beam. As in the HEBT, the loss will be localized in the two or three cells downstream from the collimators. These losses are of the order of $10 \cdot 10^{-8}$.

One should include in this section the losses in the target window due to nuclear scattering.

4 Summary

The following tables summarize the results discussed along the note. Beam losses are classified attending to the mechanism producing the loss. Table 2 shows the controlled loss distribution among collimation systems and dumps. Table 3 includes the uncontrolled loss mechanisms along the accelerator chain.

Mechanism	Location	Fraction	Energy	Power
FRONT END				
Unbunched beam	LEBT chopper	$27.7 \cdot 10^{-2}$	0.065 MeV	36 W
Unbunched beam	MEBT chopper	$4.3 \cdot 10^{-2}$	2.5 MeV	215 W
HEBT				
H^0 Ionization at the Linac	Linac Dump	$1.0 \cdot 10^{-5}$	≤ 1 GeV	20 W
Linac transverse tails	x-y collimator	$1.0 \cdot 10^{-5}$	1 GeV	20 W
Energy jitter/spread	z collimator	$1.0 \cdot 10^{-3}$	1 GeV	2.0 kW
RING				
Beam in gap	collimator	$1.0 \cdot 10^{-4}$	1 GeV	200 W
Excited H^0 at foil	collimator	$1.3 \cdot 10^{-5}$	1 GeV	26 W
Partial ioniz. and foil miss	Injection dump	$1.0 \cdot 10^{-2}$	1 GeV	20 kW
Space-charge halo	Collimator	$1.9 \cdot 10^{-3}$	1 GeV	3.8 kW
Energy straggling at foil	Collimator	$3.0 \cdot 10^{-6}$	1 GeV	6 W
RTBT				
Kicker misfire	Collimator	$1.0 \cdot 10^{-5}$	1 GeV	20 W

Table 2: Estimated controlled losses along the accelerator chain. Losses are given as a fraction of the total beam. The detailed distribution of the losses is given in the corresponding section and references.

Table 4 list the total losses expected under normal operation starting on the front end till the target. Figure 5 shows the same distribution. The ring starts at the beginning of the injection straight section and finishes at the end of arc D.

Mechanism	Location	Fraction	Energy [MeV]	Length [m]	Power [W/m]
FRONT END					
RFQ transmission	Uniform	$2.0 \cdot 10^{-1}$	≈ 0.75	3.7	80.7
DTL					
Emittance growth	End of Tank 1	$6.6 \cdot 10^{-5}$	2.5 - 7.5	4.2	0.24
Emittance growth	End of Tank 2	$2.42 \cdot 10^{-5}$	7.5 - 22	6.1	0.18
CCL					
Double H^- stripping	CCL module 1	$1.9 \cdot 10^{-5}$	86.5 - 107	12	0.35
Emittance growth	CCL module 1	$4.7 \cdot 10^{-5}$	86.5 - 107	12	0.86
SCL					
Emittance growth	Warm sections	$3.7 \cdot 10^{-6}$	≤ 1000	37	≤ 0.2
Emittance growth	Supl. 9 periods	$1.24 \cdot 10^{-5}$	≤ 1000	71	0.35
HEBT					
Collimator outscattering	Achromat	$7.5 \cdot 10^{-6}$	1000	15	0.1
RING					
Magnetic H^- stripping	INJB2	$1.3 \cdot 10^{-7}$	1000	1	0.3
Nuclear scattering at foil	Foil	$3.7 \cdot 10^{-5}$	1000	30	2.5
Collimator inefficiency	All ring	$1.0 \cdot 10^{-4}$	1000	218	0.9
RTBT					
Nuclear scatt. at window	Window	$4.0 \cdot 10^{-2}$	1000	–	

Table 3: Uncontrolled loss budget along the accelerator chain depending on the loss mechanism. Losses produced by H^- stripping are not considered here. Smaller losses in the accelerating are not indicated here and can be found in reference [7]

Location	Fractional loss	Length [m]	Beam power [W/m]	Energy [MeV]
LEBT chopper	$2.8 \cdot 10^{-1}$	–	36	0.065
RFQ	$2.0 \cdot 10^{-1}$	3.7	80.7	≈ 0.75
MEBT	$1.1 \cdot 10^{-3}$	3.6	1.56	2.5
MEBT chopper	$4.3 \cdot 10^{-2}$	–	215	2.5
DTL Tank 1	$3.0 \cdot 10^{-4}$	4.2	0.72	2.5 - 7.5
DTL Tank 2	$1.5 \cdot 10^{-4}$	6.1	0.72	7.5 - 22
DTL Tank 3	$4.8 \cdot 10^{-5}$	6.3	0.47	22 - 40
DTL Tank 4	$2.9 \cdot 10^{-5}$	6.4	0.44	40 - 56.6
DTL Tank 5	$2.2 \cdot 10^{-5}$	6.3	0.45	56.6 - 72.5
DTL Tank 6	$1.7 \cdot 10^{-5}$	6.3	0.44	72.5 - 87
CCL Module 1	$8.0 \cdot 10^{-5}$	12	1.32	87 - 107
CCL Module 2	$1.9 \cdot 10^{-5}$	13	0.35	107 - 131
CCL Module 3	$1.8 \cdot 10^{-5}$	14	0.36	131 - 157
CCL Module 4	$2.4 \cdot 10^{-5}$	15	0.55	157 - 185
SCL Low β	$1.8 \cdot 10^{-6}$	18	0.06	185 - 379
SCL High β	$1.9 \cdot 10^{-6}$	19	0.14	379 - 1000
Suppl. 9 periods	$1.2 \cdot 10^{-5}$	71	0.35	1000
Linac dump	$1.0 \cdot 10^{-5}$	–	20	≤ 1000
HEBT	$2.8 \cdot 10^{-5}$	169.5	0.3	1000
HEBT x-y-collimators (2)	$1.0 \cdot 10^{-5}$	–	20	1000
HEBT Achr	$7.5 \cdot 10^{-7}$	15	0.1	1000
HEBT z-collimator	$1.0 \cdot 10^{-3}$	–	2000	1000
INJB2	$1.3 \cdot 10^{-7}$	1	0.3	1000
Injection	$3.7 \cdot 10^{-5}$	30	2.5	1000
Injection dump	$1.0 \cdot 10^{-2}$	–	20000	1000
Ring collimators (3)	$1.9 \cdot 10^{-3}$	–	3800	1000
Ring	$1.0 \cdot 10^{-4}$	218	0.9	1000
RTBT collimators (2)	$1.0 \cdot 10^{-5}$	–	20	1000

Table 4: Loss budget along the accelerator chain according to location. Controlled losses are indicated in bold face and have no length parameter.

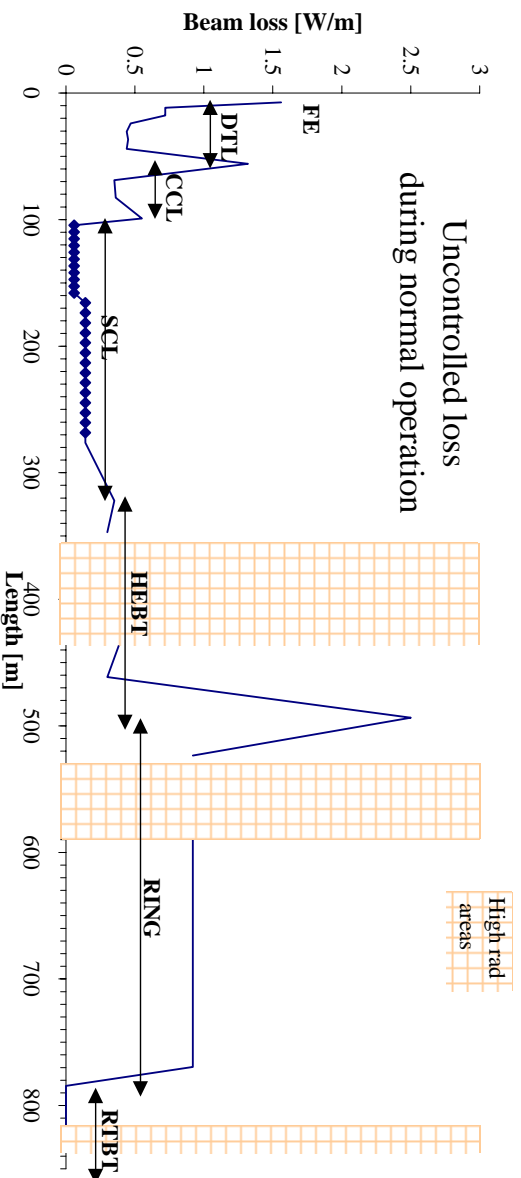


Figure 5: Uncontrolled loss approximate distribution along the accelerator chain from the front end to the target. High radiation areas are excluded from the plot. Dots in the SCL indicate that the loss occurs only in the 1.6 m warm section.

References

- [1] Proceedings of the 7th ICFE Mini-Workshop on High Intensity, High-brightness Beams, Lake Geneva, Sept 1999
- [2] "Collimation in the HEBT" D. Raparia et al. SNS/BNL Technical note 65
- [3] DOE review July 1999
- [4] ASAC review/September 2000
- [5] "The SNSNS ring to target beam transport line" D. Raparia. SNS/BNL Technical note 6
- [6] "Beam loss from H^- stripping in the residual gas" TN LANSCE- 1:99-085
- [7] "Beam loss in the SNS linac" E. Tanke et al. SNS Technical memo 16-March-2001
- [8] "Beam loss and activation at LANSCE and SNS" B. Hardekopf. See ref. [1]
- [9] "Simulated performance of the superconducting sections of the APT linac under various fault and error conditions" E.R. Gray, S. Nath and T. Wangler. PAC'97 Vancouver
- [10] "SNS Linac Activation: Codes and Experience" T. Wangler
- [11] "Impact of the Superconducting Linac on the HEBT and Ring", D. Raparia et al. SNS/BNL Technical note 70